J. Biochem. 2009;145(5)677–684
doi:10.1093/jb/mvp025

Characterization of Type I Collagen Fibril Formation Using Thioflavin T Fluorescent Dye

Koichi Morimoto*, Kazuya Kawabata, Saori Kunii, Kaori Hamano, Takuya Saito and Ben'ichiro Tonomura

Department of Biotechnological Science, Kinki University, Kinokawa, Wakayama 649-6493, Japan

Received January 27, 2009; accepted January 28, 2009; published online February 9, 2009

Collagen is composed of fibrils that are formed by self-assembly of smaller units, monomers which are triple-helical polypeptide. However, the mechanism of fibril formation at the level of individual molecules has remained to be clarified. We found that the fluorescence of thioflavin T, which has been widely used as a specific dye for amyloid fibrils, also increased by binding with fibrils of atelocollagen prepared from yellowfin tuna skin. There was a linear correlation between the fluorescence increase and the amount of atelocollagen within a collagen concentration range of 0–0.15 mg/ml at pH 6.5 with 50 μM thioflavin T. In contrast, neither actinidain-processed collagen that keeps monomeric nature nor heat-denatured collagen could cause the fluorescence increase of thioflavin T at all. The relationship between the fluorescence increase and thioflavin T concentration was fit to a theoretical binary binding curve. An apparent dissociation constant, K_d, and a maximal fluorescence increase, ΔF_{max}, were calculated at various pHs. The values of K_d and ΔF_{max} were dependent on pH (K_d was 9.4 μM at pH 6.5). The present finding demonstrates that thioflavin T specifically binds to collagen fibrils and may be used as a sensitive tool for the study of collagen structure.

Key words: collagen, fibril formation, thioflavin T, fluorescence.

Abbreviations: AP-collagen, actinidain-processed collagen; SEM, scanning electron microscopy; Th-T, thioflavin T; T_m, melting temperature.

Self-assembly of proteins is a well-known phenomenon of biological processes. Collagen, the primary structural element in the extra-cellular matrix, has specific functions in physiological events, such as cell proliferation and differentiation. Type I collagen especially is an abundant protein *in vivo*, and its structure is highly ordered. Type I collagen is composed of monomers that are heterotrimer of two α1 and one α2 chains folded into triple helical structure (*1–4*). They spontaneously aggregate into fibrils and then into fibres. There are numerous reports concerning the formation of collagen fibrils (*1–11*). In connective tissue, some of each collagen chain form covalently cross-linked fibrils to add mechanical strength in itself and network stability (*12*). Since collagen forms fibrils spontaneously by self-assembly to give oriented D-staggered striates, which can be observed using scanning electron microscopy (SEM) and transmittance electron microscopy (*13–15*), the specific axial and azimuthal association is an intrinsic feature of the collagen-fibril formation. However, the molecular mechanism of the fibril formation remains to be elucidated. The pepsin-hydrolysed collagen, namely atelocollagen, as well as the acid-soluble collagen forms fibril assemblies although the atelocollagen lacks β-turn hairpin loop structure of N-telopeptide (*16*). The triple helical structure of collagen is essential to recognize each other and to form the fibril assemblies. The kinetics of fibril formation was studied using turbidity measurements, which required high purity and concentration of the samples (*3*). The turbidity-time curve shows a lag phase, a propagation phase and a plateau, and depends on temperature. However, the molecular mechanisms in the lag and propagation phases have not been elucidated (*3*).

For histological studies of the extra-cellular matrix, several acid dyes, such as picrosirius red and von Gieson's picrofuchsin, were used (*17*, *18*). Since their specificity for collagen fibril was low, an anti-collagen antibody labelled with fluorescence dye has generally been used for specific staining. Thioflavin T (Th-T) is a sulphur-containing compound and has been widely used as a specific dye for the detection and characterization of amyloidogenesis *in vitro* (*19–24*). Although various amyloid fibrils have been stained with fluorescent dyes, the fluorescence of bound Th-T is particularly important in distinguishing between the monomer molecule and the fibril of amyloid (*25–29*). Khurana *et al*. (*23*) suggested that the fluorescence of Th-T bound to amyloid fibrils depended on the micelle concentration and micelle formation. There are no previous reports on the analysis of collagen-fibril formation using Th-T.

Recently, several experiments showed the interaction between collagen fibril and amyloid fibril (*30*, *31*). However, the binding sites of both fibrils are still not clear. In addition, collagen fibril enhances the amyloid deposition under physiological conditions (*32*). This event might be considered as a favourable substitution of

*To whom correspondence should be addressed. Tel: +81-736-77-3888, Fax: +81-736-77-4754,
E-mail: morimoto@waka.kindai.ac.jp

intermolecular packing that led to the heterotypic fibrils. Although the structures of these fibrils are quite different, the electrostatic and hydrophobic properties might be similar among some parts of the fibrils because surface of fibril molecule plays a definite role in the specific recognition and ordering interactions.

In this study, we demonstrate that under suitable conditions Th-T can be bound to atelocollagen fibril purified from yellowfin tuna (*Thunnus albacares*) skin. The atelocollagen was found as type I, and the triple helical structure and the formation of fibril were confirmed by CD spectroscopy, SDS–PAGE and SEM. Binding of Th-T to atelocollagen fibril at various pHs was measured by fluorescence spectroscopy. To examine the binding of Th-T to monomeric collagen, we also prepared actinidain-processed collagen by using actinidain, a peptidase from kiwi fruits (*33*, *34*). Actinidain-processed collagen, which was named AP-collagen, keeps the triple-helical structure composed of three α-chains but lacks the covalently cross-linked β-chain and γ-chain. It is thought that AP-collagen retains as the monomeric nature. In contrast, the atelocollagen has a significant amount of the cross-linked chains, β-chain and γ-chain. The cross-linked collagen molecules would have a great influence on fibril formation. An apparent dissociation constant for the binding of Th-T and atelocollagen and the maximal fluorescence increase were estimated at various pHs. We found that the collagen fibril formation could be monitored with Th-T fluorescence similarly to the case of amyloid fibril formation.

MATERIALS AND METHODS

Preparation of Collagens from Yellowfin Tuna Skin—The atelocollagen and AP-collagen were prepared from yellowfin tuna according to the method of Morimoto *et al*. (*34*). Crude acid-soluble collagen was treated with 30 U/ml (final concentration) of porcine pepsin (Sigma–Aldrich, MO, USA) or 1% (w/v) of actinidain, and then incubated with stirring at 4°C for 3 days, respectively. Proteins were salted out by adding NaCl to give a final concentration of 2.5 M. Each precipitate was dissolved in 20 mM acetate buffer (pH 4.0) and then dialysed against ultra-pure water to remove the smaller proteolytic products. Atelocollagen and AP-collagen were lyophilized and stored at –80°C. The concentration of each collagen solution was estimated from the weight of the lyophilized preparation.

CD Spectroscopy of Atelocollagen—The triple-helical structure of the purified collagen molecule was confirmed by CD spectrum as reported previously (*34*). The Far-UV CD spectrum of atelocollagen was measured by scanning through the range of 205–250 nm with a CD spectrophotometer, J-600 (Jasco, Tokyo, Japan). Measurements were carried out using a 1.0 mg/ml solution of atelocollagen in 40 mM acetate buffer (pH 4.0) or 40 mM phosphate buffer (pH 6.5) in a quartz cell with a 0.1-cm optical path length. Each CD spectrum at pH 4.0 in Fig. 1 was the average of three measurements. The CD_{222} values at pH 4.0 and pH 6.5 were monitored at different temperatures ranging from 10°C to 50°C. The thermal denaturation curve was analysed with the CD ratio determined by the equation: CD ratio (%) = $100 \times (CD_T - CD_{50°C})/(CD_{10°C} - CD_{50°C})$, where the suffix indicates the temperature of measurement.

Centrifugal Fractionation and SDS–PAGE of Atelocollagen Fibril—Atelocollagen (0.5 mg/ml) was incubated to form fibril in 40 mM acetate buffer (pH 4.0-5.5) or 40 mM phosphate buffer (pH 6.0–6.5) for 7 days at 20°C. The atelocollagen fibril formed under various pH conditions was centrifuged down at 14,000*g* for 20 min. The precipitate and the supernatant fractions were analysed by 5% SDS–PAGE under reducing conditions (*35*), and collagen chains were stained with Coomassie brilliant blue R-250. The percentage of collagen chains in the precipitate fraction was determined colourimetrically by an Image Master 2D Elite version 2.00 (Amersham Bioscience Corp., NJ, USA).

SEM of Atelocollagen Fibrils—A sample of atelocollagen (3 mg/ml in 40 mM phosphate buffer, pH 6.5, incubated for 7 days at 20°C) was placed on a plastic cell disk LF (Sumitomo Bakelite, Tokyo, Japan). Specimen on the cell disk was fixed with 2% glutaraldehyde for 4 h at 4°C, and then rinsed twice in distilled water. Sample was dehydrated with a graded series of ethanol. After treatment with isoamyl acetate, the specimen was dried in a critical-point drying apparatus (HCP-1; Hitachi Koki, Tokyo, Japan) with liquid carbon dioxide. The dried sample was coated with a 3-nm-thick layer of platinum-palladium by evaporation in a magnetron sputter coater (E-1030; Hitachi, Tokyo, Japan). The morphological observation of atelocollagen fibrils was carried out with an S-900 ultra-high-resolution scanning electron microscope (Hitachi, Tokyo, Japan) with an accelerating voltage of 10 kV.

Fluorescence Spectroscopy of Thioflavin T Bound with Atelocollagen Fibrils—Emission fluorescence spectra of Th-T, atelocollagen and the mixure of Th-T and atelocollagen were observed by using an RF-5300PC spectrofluorometer (Shimadzu, Kyoto, Japan) at 20°C. Similarly, those of the mixure of Th-T and heat-denatured atelocollagen (incubation for 30 min at 60°C) were monitored under the same conditions. To measure the dose dependence of the fluorescence spectra, 50 μl of Th-T (final conc. to be 50 μM) was added to 950 μl of atelocollagen (final conc. to be 0, 0.03, 0.06, 0.09, 0.12 or 0.15 mg/ml) at pH 6.5 and the samples were then incubated for 8 min at 20°C. Th-T fluorescence was measured with excitation at 430 nm and emission at 485 nm according to the previously described method with some minor modifications (*22*). The fluorescence increase at 485 nm was determined by subtracting, from the fluorescence intensity of the mixture of Th-T and atelocollagen, the background fluorescence of Th-T and collagen separately dissolved in the same buffer. On the other hand, to examine the effects of Th-T concentration on the fluorescence spectra at a fixed concentration of atelocollagen, 50 μl of Th-T (final conc. to be 0, 5, 10, 15, 20, 30, 40, 50 or 60 μM) was added to 950 μl of atelocollagen (final conc. to be 0.15 mg/ml). The fluorescence intensity was measured at pH 4.0, 4.5, 5.0, 5.5, 6.0 and 6.5, using 40 mM acetate buffer (pH 4.0-5.5) or 40 mM phosphate buffer (pH 6.0-6.5), respectively. In order to examine the binding of Th-T to the monomeric collagen, we measured the

fluorescence spectra of Th-T, AP-collagen, the mixture of Th-T and AP-collagen and the mixture of Th-T and heat-denatured AP-collagen at pH 4.0. The experimental conditions with AP-collagen were the same as those with atelocollagen.

An apparent dissociation constant, K_d, of the interaction between Th-T and a binding site, and the maximum fluorescence increase, ΔF_{max}, at each pH was obtained from a theoretical fitting of the plot of fluorescence increase ΔF *versus* $[\text{Th-T}]_0$, the initial concentration of Th-T, with a Kaleida Graph software (Synergy Software, Reading, PA, USA), where $\Delta F = \Delta F_{max} \cdot [\text{Th-T}]_0/(K_d + [\text{Th-T}]_0)$. Here, $\Delta F = \Delta f \cdot [\text{Th-T}]_B$ and $\Delta F_{max} = \Delta f\ [\text{B.S.}]_T$, where the definition of each component is the following: $[\text{Th-T}]_B$ is the concentration of Th-T bound to atelocollagen; $[\text{B.S.}]_T$ is the total concentration of the Th-T-binding site on atelocollagen; $\Delta f = f_B - f_0$; f_B is the apparent fluorescence coefficient for the bound form Th-T and f_0 is the one for free Th-T. Accordingly, ΔF_{max} represents the fluorescence increase expected when all the binding sites are fully occupied by Th-T, whose concentration is expressed as $[\text{Th-T}]_{max}$.

RESULTS

CD Spectra and Thermal Stability of Atelocollagen—The CD spectra of atelocollagen at pH 4.0 are shown in Fig. 1. The maximum positive CD value of atelocollagen at 10°C was obtained at 222 nm, which is a unique feature of a triple helical structure (*36*). However, the CD spectrum at 50°C corresponded to that of a random coil. This demonstrates that tuna atelocollagen contains a triple-helical structure at 10°C and has lost it at 50°C. The melting temperature (T_m) of atelocollagen at pH 4.0 and pH 6.5, marked by a 50% CD ratio of the thermal denaturation curve, was estimated to be 31°C and 36°C, respectively (Fig. 1, inset). Measurements of the CD_{222} value indicated that the triple-helical form of collagen was stable below 25°C, and subsequent experiments were carried out at 20°C unless otherwise mentioned. Accordingly, the heat-denatured atelocollagen was prepared by incubating a collagen solution for 30 min at 60°C.

Evaluation of Atelocollagen Fibril by Centrifugation and SDS–PAGE—The soluble and insoluble fractions of atelocollagen solution in various pH conditions were separated by centrifugation, and those fractions were evaluated by SDS–PAGE (*11*). Figure 2A and B show 5% SDS–PAGE of the supernatant fraction and the precipitate fraction, respectively. In those SDS–PAGE patterns, β11-chain is dimer consisted of two α1-chains, β12-chain is dimer consisted of one α1-chain and one α2-chain and γ-chain is trimer consisted of two α1-chains and one α2-chain. The atelocollagen chains at pH 4.0-5.5 were mainly found in the supernatant fraction, whereas the atelocollagen chains at pH 6.0–6.5 were mostly found in the precipitate fraction. The percentages of the precipitate fraction at pH 6.0 and pH 6.5 were estimated 83% and 94% (Fig. 2B), respectively. A significant amount of the atelocollagen fibril was present in the precipitate fraction. Since the fibril formation of the atelocollagen is a pH-dependent process, at pHs 6.0 and 6.5, most of the atelocollagen must be in the form of fibril that is low in solubility.

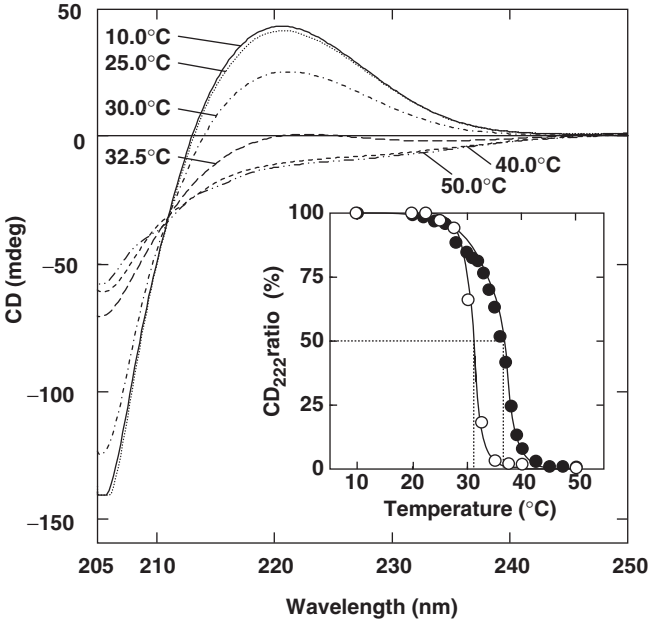

Fig. 1. **CD spectra of atelocollagen in the Far-UV region.** The spectra were measured as described in 'MATERIALS AND METHODS' section. The CD spectra of atelocollagen at pH 4.0 were recorded at temperature from 10 to 50°C. The heat denaturation curve of atelocollagen at pH 4.0 (open circle) and pH 6.5 (closed circle) are shown in the inset.

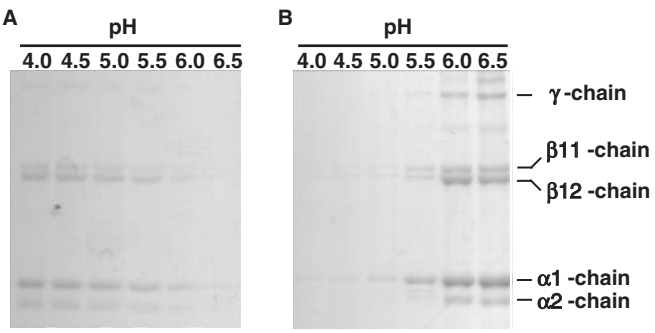

Fig. 2. **Centrifugal fractionation and 5% SDS–PAGE of atelocollagen at various pHs.** Atelocollagen was fractionated by centrifugation (14,000*g*, 20 min, 20°C). The supernatant and the precipitate fractions were analysed by 5% SDS–PAGE. (A) Supernatant fractions; (B) precipitate fractions.

SEM of Atelocollagen Fibrils—An electron micrograph of atelocollagen prepared at pH 6.5 clearly showed microfibril assemblies with a typical D-periodic staggered structure of 67 nm (Fig. 3). The diameter of the collagen fibrils ranged from 38 to 76 nm. The average diameter was estimated to be 57 nm. Therefore, the atelocollagen purified from yellowfin tuna skin spontaneously forms fibrils at neutral pH *in vitro*. This is in good agreement with previous reports on collagen of other sources (*13–15*).

Fluorescence Spectroscopy of Th-T Bound with Atelocollagen Fibrils—Figure 4A and B show the fluorescence spectra of Th-T, atelocollagen, the mixture of Th-T and atelocollagen and the mixture of Th-T and heat-denatured atelocollagen at pH 4.0 and pH 6.5, respectively. Th-T bound to atelocollagen fibrils exhibited enhanced fluorescence emission at 485 nm with excitation at 430 nm at both pH. No enhancement in Th-T fluorescence was observed for the mixture with heat-denatured atelocollagen either at pH 4.0 or 6.5. As shown in Fig. 4C, no increase of Th-T fluorescence was observed at all in the mixture with AP-collagen or heat denatured AP-collagen at pH 4.0. We also confirmed that Th-T itself had the same fluorescence spectrum at pH range of 4.0 to 6.5.

The fluorescence-intensity increase of Th-T, ΔF, was proportional to the atelocollagen fibril concentration as shown in Fig. 5. A linear relationship of ΔF was observed between 0 and 0.15 mg/ml atelocollagen in the presence of 50 μM Th-T. The fluorescence emission of Th-T in the presence of 0.15 mg/ml atelocollagen at pH 6.5 increased by increasing Th-T concentration and became saturated at above 50 μM (Fig. 6A). The plot of ΔF *versus* initial Th-T concentration fit to a theoretical binary binding

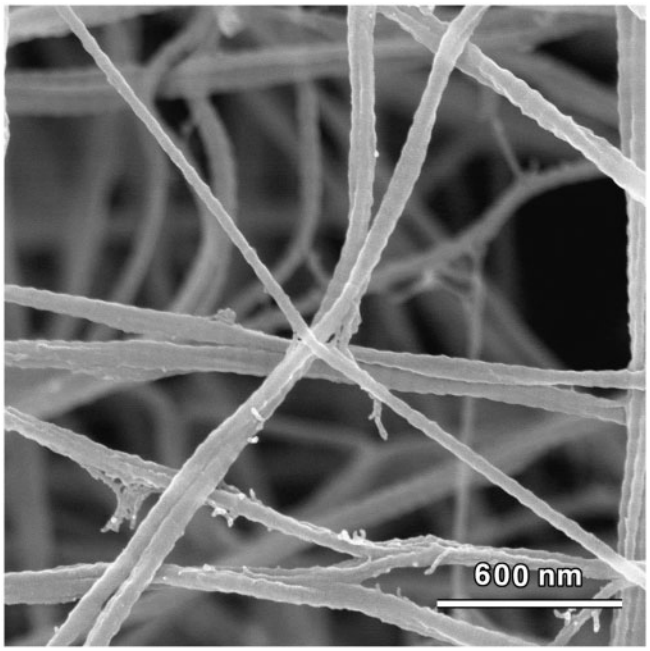

Fig. 3. **Scanning electron micrographs of atelocollagen at pH 6.5.** SEM was performed as described in 'MATERIALS AND METHODS' section. The bar represents 600 nm.

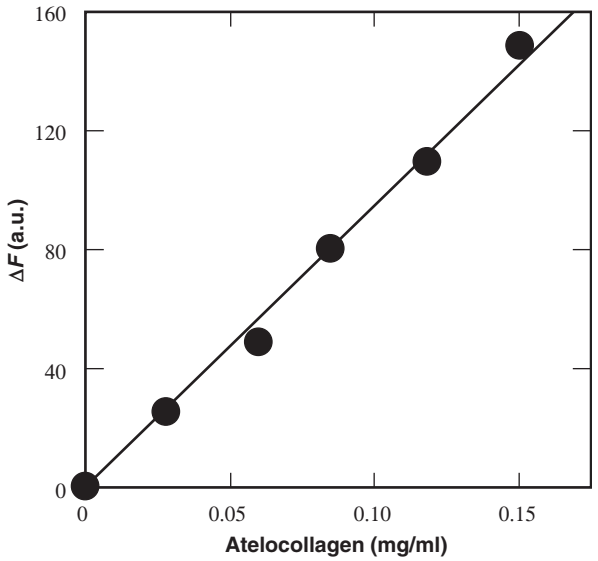

Fig. 5. **A linear relationship between the bound form of Th-T and atelocollagen concentration as observed by fluorescence change.** A solution of Th-T (final conc. to be 50 μM) was added to various concentrations of atelocollagen (final conc. to be 0–0.15 mg/ml) and the increase in fluorescence intensity, ΔF, was measured. Excitation was at 430 nm and emission was detected at 485 nm.

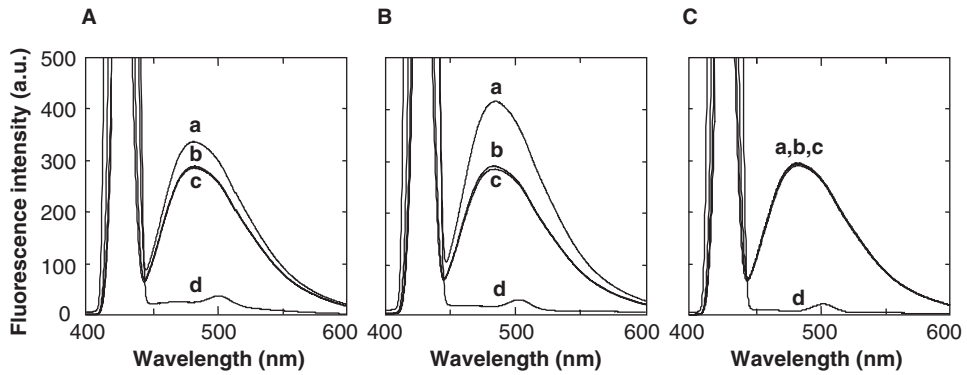

Fig. 4. **Fluorescence emission spectra of Th-T mixed with atelocollagen or AP-collagen.** (A) Fluorescence spectra of Th-T with atelocollagen at pH 4.0 (40 mM acetate buffer); (B) fluorescence spectra of Th-T with atelocollagen at pH 6.5 (40 mM phosphate buffer); (C) fluorescence spectra of Th-T with AP-collagen at pH 4.0 (40 mM acetate buffer). In each frame, curve 'a' represents the fluorescence of the mixture of Th-T and each collagen preparation; curve 'b', that of the mixture of Th-T and heat-denatured preparation of each collagen; curve 'c', that of Th-T only; and curve 'd', that of each collagen preparation only. Excitation was at 430 nm and the slit width for the excitation and emission was 10 nm. The large peak around 430 nm is due to the scattering of the excitation light.

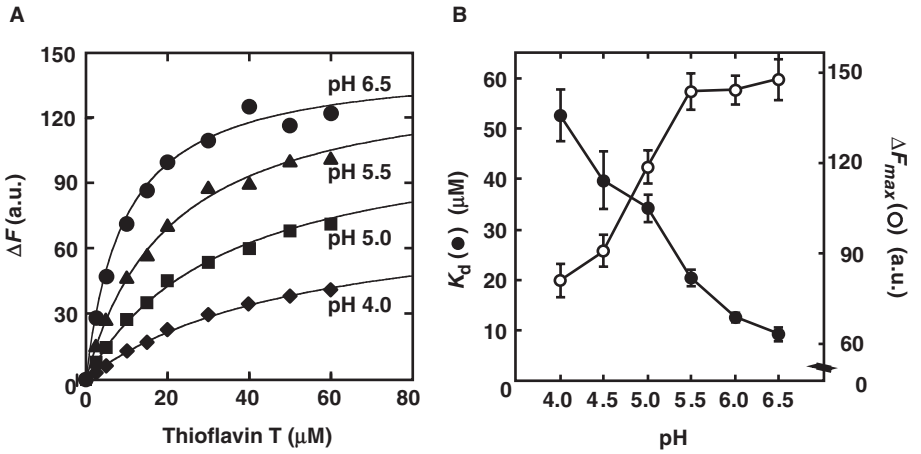

Fig. 6. **The effects of Th-T concentration and pH on the fluorescence increase upon the binding with atelocollagen.** Excitation was at 430 nm and emission was detected at 485 nm. The reaction was performed by adding a Th-T solution (final conc. to be 0–60 μM) to an atelocollagen solution (final conc. to be 0.15 mg/ml) at various pHs at 20°C. (A) The solid lines are the best-fit theoretical curves of a binary-binding equation: $\Delta F = \Delta F_{max}\ [\text{Th-T}]_0/(K_d+[\text{Th-T}]_0)$ (see 'MATERIALS AND METHODS' section). (B) The K_d and the ΔF_{max} values at various pHs (pH 4.0–6.5) were calculated from the theoretical curves. Vertical bars indicate the standard errors. For pH 6.0 and 6.5, 40 mM phosphate buffer was used, and 40 mM acetate buffer for pHs 4.0–5.5.

equation (see 'MATERIALS AND METHODS' section), and an apparent dissociation constant, K_d, and a maximum fluorescence increase, ΔF_{max}, for Th-T·atelocollagen interaction was estimated. Thus, it can be considered that Th-T specifically binds to the atelocollagen fibril. The similar measurements were made also at pHs 4.0–6.5 (Fig. 6A). Figure 6B shows the effects of pH on K_d and ΔF_{max}. It was assumed that ΔF is proportional to the concentration of Th-T bound to the collagen fibrils (see 'MATERIALS AND METHODS' section). The greatest enhancement in fluorescence was observed at neutral pH. The relationship of ΔF_{max} values *versus* pH (Fig. 6B) shows that the fibril formation is a pH-dependent process and may be correlated with a group having a pK_a of *ca*. 4.8.

DISCUSSION

Preparations of Collagen—The triple-helical structure and the fibril formation of the tuna atelocollagen were examined by CD (Fig. 1), centrifugal fractionation (Fig. 2) and SEM (Fig. 3). The reconstitution of collagen fibrils *in vitro* has been investigated extensively (*7*). Most researchers have simply extracted acid-soluble collagen from connective tissues and studied the mechanism of fibril formation by neutralizing or warming the solution (*1–3*). However, reproducibility of fibril formation has always been an issue when using collagens extracted in this way. In order to examine fibril formation of collagen *in vitro* in a more reproducible manner, we obtained atelocollagen by hydrolysis with pepsin (*16*). As expected, atelocollagen proved to be highly soluble and less viscous at acidic pH. Since temperature strictly affects the triple-helical structure and the fibril formation of collagen, we analysed the thermal stability of the secondary structures in atelocollagen by CD. As shown in Fig. 1, the typical triple-helical structure was maintained at pH 4.0, 20°C. Since the collagen forms fibrils under physiological conditions, we initially examined the stable temperature and the T_m of the triple-helical structure. The tuna atelocollagen maintained fully the triple-helical structure below 25°C. The T_m was found to be 36°C at pH 6.5, which was relevant to the temperature of living circumstance of tuna, *ca*. 28°C. The T_m at pH 4.0 was about 31°C. Thus, we concluded that 20°C was good enough to keep the atelocollagen stable. The CD spectra (Fig. 1) suggest that heat-denatured atelocollagen is in a completely random conformation.

Consistent with the previous observations (*1–6*), pH has a great influence on the fibril formation of atelocollagen. Judging by SDS–PAGE (Fig. 2), it is thought that large parts of atelocollagen at pH 6.0–6.5 were in the form of fibril and precipitated by centrifugation. To confirm the fibril formation of atelocollagen at pH 6.5, we observed atelocollagen self-assembly by SEM, and examined the size distribution and the shape of the fibrils. The atelocollagen fibrils showed a well-defined shape with typical D-periodic structures (Fig. 3), which is consistent with other published data (*13–15*). Since the atelocollagen prepared by our methods formed a narrow distribution of relatively small diameter (38–76 nm), presumably it is suitable for the analysis of fibril formation. The large-size distribution might have a significant influence on accuracy and reproducibility of measurements.

On the other hand, we chose AP-collagen preparation (*34*) as a reference. We demonstrated in the previous report (*34*) that AP-collagen of tuna had the triple helical structure made of α1- and α2-chains, whose molecular size were similar to those of atelocollagen, but that AP-collagen exhibited no β or γ band on SDS–PAGE, indicating absence of inter-strand cross-links which was a prerequisite for fibril formation. SEM of AP-collagen (to be published elsewhere) showed completely different

superstructure from that of atelocollagen. It is thought that the AP-collagen keeps the monomeric nature at pH 4.0.

Fluorescence of Th-T Bound to Atelocollagen—Some increase was observed in Th-T fluorescence when mixed with atelocollagen at pH 4.0 (Fig. 4A), whereas AP-collagen had no effects on fluorescence change of Th-T (Fig. 4C). The fluorescence increase of Th-T upon binding to atelocollagen was specific to fibril structure rather than to the triple helical structure. It was shown that covalently cross-linked atelocollagen chains could act as structural nuclei that were essential for further growth of fibrils (*37*), and the existence of those chains at pH 4.0 in tuna atelocollagen were suggested by β and γ band of SDS–PAGE (Fig. 2A), whereas there were detected no those bands in AP-collagen (*34*). The cross-linked chains contained in the atelocollagen at pH 4.0 are presumably relevant to the fluorescence change. The ΔF was larger at pH 6.5 (Fig. 4B, curve a), and this is consistent with the indication by the centrifugal study that a large fraction of atelocollagen was fibril at this pH (Fig. 2B). We confirmed that the heat-denatured preparations of atelocollagen and AP-collagen showed no effects on the Th-T fluorescence enhancement (Fig. 4, curve b). The intrinsic fluorescence intensity of Th-T (Fig. 4, curve c) was very similar each other within the pH range tested, 4.0–6.5. This agrees with other observations (*24*). Naiki *et al*. (*21*) reported that Th-T bound to β-amyloid fibrils fluoresced at 482 nm with an excitation at 450 nm. Wisniewski *et al*. (*38*) reported that the excitation and the emission wavelengths of Th-T bound to β-amyloid fragments β(*1–40*) were 435 nm and 485 nm, respectively.

In order to examine proportional relationship in the binding of Th-T to atelocollagen, we measured ΔF at 0–0.15 mg/ml atelocollagen in the presence of 50 μM Th-T. There was a linear relation between ΔF and atelocollagen concentration (Fig. 5). While the intrinsic fluorescence of Th-T in the pH range of 4.0–6.5 showed similar intensity as stated above, the fluorescence of Th-T bound to atelocollagen fibril clearly showed pH dependence (Figs 4A, 4B and 6A). A theoretical curve was in good agreement with the experimental plots of ΔF *versus* initial Th-T concentration at each pH (Fig. 6A). These results together indicate that Th-T binds specifically to atelocollagen fibrils. From the theoretical curves, we obtained $K_d \pm$ standard error (μM) and $\Delta F_{max} \pm$ standard error (arbitrary units) at various pHs. The K_d and the ΔF_{max} at pH 6.5, for example, were 9.4 ± 1.4 μM and 146 ± 7.4 a.u., respectively (Fig. 6B). Naiki *et al*. (*21*) reported that the K_d value for amyloid fibril and Th-T was estimated to be 0.76 μM. Similarly, the K_d values for the synthetic β/A4-derived peptides β(*1–28*) and β(*1–40*), the Alzheimer's disease-associated peptides, were 0.54 μM and 2 μM, respectively (*22*). Presently, we have found that Th-T has a lower affinity for the atelocollagen fibril than for the amyloid fibril.

The ΔF_{max} increased about 2-fold by shifting from pH 4.0 to pH 6.5 and reached a plateau at above pH 5.5 (Fig. 6B). The increase in the ΔF_{max} at neutral pH was consistent with the results of centrifugal fractionation proven by SDS–PAGE (Fig. 2B). The value of ΔF_{max} can be regarded as the product of an apparent fluorescence coefficient difference, Δf ($=f_B - f_0$), and maximal concentration of Th-T bound to atelocollagen fibrils, $[\text{Th-T}]_{max}$ (see 'MATERIALS AND METHODS' section). Since we confirmed that the intrinsic fluorescence of Th-T was the same in the pH range of 4.0–6.5, the pH profile of ΔF_{max} in this pH region (Fig. 6B) cannot be explained in terms of f_0 values. Alternatively, the value of f_B might have correlated with the binding strength of Th-T to atelocollagen fibril: the stronger the binding, the larger f_B value. However, a feature of Fig. 6B that ΔF_{max} reaches almost a plateau in pH range 5.5–6.5 where the value of K_d continues to decrease seems to exclude this possibility. Accordingly, it is most likely that the pH profile of ΔF_{max} represents that of $[\text{Th-T}]_{max}$, which in turn corresponds to $[\text{B.S}]_T$, the total concentration of the Th-T-binding site that accompanies fibril formation. An apparent pK_a of an ionizing group that may control the atelocollagen fibril formation is estimated to be about 4.8 from Fig. 6B. This ionizing group could be a carboxyl moiety of the atelocollagen. Indeed, the C-telopeptide of the α1 chain that contains acidic amino acid residues, Glu and Asp, has been reported to play an important role in the molecular recognition of collagen molecules (*10*).

In the scanning electron micrograph, the tuna atelocollagen fibrils exhibited the D-periodic banding pattern of 67 nm and molecular packing in small diameter of 57 nm (Fig. 3B). In collagen fibrils, a hole or gap zone is positioned in the region between the N-terminal end of one molecule and the adjacent C-terminal end of the next molecule (*4*, *8*, *14*). Collagen fibrils are formed by binding monomers along the fiber axis so that each monomer slides in turn in the axial direction with a regular spacing. It is generally thought that deposits of such as calcium hydroxyapatite to collagen fibrils occur at the gap region (*18*). Similarly, the presence of a hole or gap region may facilitate the binding of Th-T to collagen fibril. No fluorescence increasing in the mixture of Th-T and AP-collagen would support this hypothesis. In the present study, this binding intensity was found sensitive to pH. The electrostatic change in the gap or hole region might be related to the interaction with the positively charged thiazole nitrogen of the Th-T micelles, which are spherical particles (3-nm diameter) (*23*, *24*). Thus, the binding affinity might be extremely sensitive to minor differences in the self-assembly conformation of these fibrils.

Interestingly, Beher *et al*. (*30*) reported that the amyloid precursor protein bound to type I collagen. Relini *et al*. (*31*) observed by atomic force microscopy that the type I collagen acted as a catalyzer for fibrillar aggregation of β2-microglobulin. At present, it is difficult to explain how type I collagen fibril interacts with β2-microglobulin fibril. However, the binding site of amyloid protein precursor to type I collagen has been identified in the COOH-terminal cyanogen bromide fragment of α1-chain, which comes into contact with a gap region (*30*, *39*). One possibility is that the binding sites of Th-T in collagen fibril might interact to the grooves of the twisted protofilament in β2-microglobulin amyloid fibril.

CONCLUSION

We have shown by using fluorescence spectroscopy for the first time that Th-T, which has been widely used as a specific dye for β-amyloid fibrils, is specifically bound to atelocollagen fibrils prepared from yellowfin tuna skin. We revealed the pH dependence of the values of K_d and ΔF_{max} in Th-T•atelocollagen interaction. This method should be useful as a sensitive tool for the study of collagen-fibril formation.

FUNDING

Grant-in-Aid for Scientific Research (16500307, K.M., partial); Grant-in-Aid for the 21st Century COE Program of the Japan MEXT; Wakayama Prefecture Collaboration of Regional Entities for the Advancement of Technological Excellence of the JST.

CONFLICT OF INTEREST

None declared.

REFERENCES

1. Gelman, R.A., Williams, B.R., and Piez, K.A. (1979a) Collagen fibril formation: evidence for a multistep process. *J. Biol. Chem.* **254**, 180–186
2. Gelman, R.A., Poppke, D.C., and Piez, K.A. (1979b) Collagen fibril formation *in vitro*: the role of the nonhelical terminal regions. *J. Biol. Chem.* **254**, 11741–11745
3. Helseth, D.L. and Veis, A. (1981) Collagen self-assembly *in vitro*. *J. Biol. Chem.* **256**, 7118–7128
4. Hulmes, D.J.S., Miller, A., White, S.W., and Doyle, B.B. (1977) Interpretation of the meridional X-ray diffraction pattern from collagen fibres in terms of the known amino acid sequence. *J. Mol. Biol.* **110**, 643–666
5. Hulmes, D.J.S., Miller, A., White, S.W., Timmins, P.A., and Berthet-Colominas, C. (1980) Interpretation of the low-angle meridional neutron diffraction patterns from collagen fibres in terms of the amino acid sequence. *Int. J. Biol. Macromol.* **2**, 338–346
6. Hulmes, D.J.S., Kadler, K. E., Mould, A.P., Hojima, Y., Holmes, D.F., Cummings, C., Chapman, J.A., and Prockop, D.J. (1989) Pleomorphism in type I collagen fibrils produced by persistence of the procollagen N-propeptide. *J. Mol. Biol.* **210**, 337–345
7. Veis, A. and George, A. (1994) Fundamentals of interstitial collagen self-assembly in *Extracellular Matrix Assembly and Structure* (Yurchenco, P.D., Birk, D.E., and Mecham, R.P., eds.) pp. 15–45, Academic Press, San Diego
8. Kadler, K.E., Holmes, D.F., Trotter, J.A., and Chapman, J.A. (1996) Collagen fibril formation. *Biochem. J.* **316**, 1–11
9. Brodsky, B. and Ramshaw, J.A.M. (1997) The collagen triple-helix structure. *Matrix Biol.* **15**, 545–554
10. Prockop, D. J. and Fertala, A. (1998) Inhibition of the self-assembly of collagen I into fibrils with synthetic peptides. *J. Biol. Chem.* **273**, 15598–15604
11. Malone, J.P., George, A., and Veis, A. (2004) Type I collagen N-telopeptides adopt an ordered structure when docked to their helix receptor during fibrillogenesis. *Proteins* **54**, 206–215
12. Eyre, D.R. and Wu, J.-J. (2005) Collagen cross-links in *Collagen* in *Top. Curr. Chem.* (Brinckmann, J., Notbohm, H., and Müller, P.K., eds.) Vol. 247, pp. 207–229, Springer-Verlag Berlin Heudelberg, Netherlands
13. Helseth, D.L., Lechner, J.H., and Veis, A. (1979) Role of the amino-terminal extrahelical region of type I collagen in directing the 4D overlap in fibrillogenesis. *Biopolymers* **18**, 3005–3014
14. Meek, K.M., Chapman, J.A., and Hardcastle, R.A. (1979) The staining pattern of collagen fibrils. *J. Biol. Chem.* **254**, 10710–10714
15. Scott, P.G. (1980) A major intermolecular cross-linking site in bovine dentine collagen involving the α2 chain and stabilizing the 4D overlap. *Biochemistry* **19**, 6118–6124
16. Sato, K., Ebihara, T., Adachi, E., Kawashima, S., Hattori, S., and Irie, S. (2000) Possible involvement of aminotelopeptide in self-assembly and thermal stability of collagen I as revealed by its removal with proteases. *J. Biol. Chem.* **275**, 25870–25875
17. Woo, H.-M., Kim, M.S., Kweon, O.-K., Kim, D.-Y., Nam, T.-C., and Kim, J.H. (2001) Effects of amniotic membrane on epithelial wound healing and stromal remodeling after excimer laser keratectomy in rabbit cornea. *Br. J. Ophthalmol.* **85**, 345–349
18. Krahn, K.N., Bouten, C.V.C., van-Tuijl, S., van-Zandvoort, M.A.M.J., and Merkx, M. (2006) Fluorescently labeled collagen binding proteins allow specific visualization of collagen in tissues and live cell culture. *Anal. Biochem.* **350**, 177–185
19. Burns, J., Pennock, C.A., and Stoward, P.J. (1967) The specificity of the staining of amyloid deposits with thioflavine T. *J. Pathol. Bacteriol.* **94**, 337–344
20. Saeed, S.M. and Fine, G. (1967) Thioflavin-T for amyloid detection. *Am. J. Clin. Pathol.* **47**, 588–593
21. Naiki, H., Higuchi, K., Hosokawa, M., and Takeda, T. (1989) Fluorometric determination of amyloid fibrils in vitro using the fluorescent dye, thioflavine T. *Anal. Biochem.* **177**, 244–249
22. LeVine, H, III. (1993) Thioflavine T interaction with synthetic Alzheimer's disease β-amyloid peptides: detection of amyloid aggregation in solution. *Protein Sci.* **2**, 404–410
23. Khurana, R., Coleman, C., Ionescu-Zanetti, C., Carter, S.A., Krishna, V., Grover, R.K., Roy, R., and Singh, S. (2005) Mechanism of thioflavin T binding to amyloid fibrils. *J. Struct. Biol.* **151**, 229–238
24. Eisert, R., Felau, L., and Brown, L.R. (2006) Methods for enhancing the accuracy and reproducibility of Congo red and thioflavin T assays. *Anal. Biochem.* **353**, 144–146
25. Naiki, H. and Nakakuki, K. (1996) First-order kinetic model of Alzheimer's β-amyloid fibril extension *in vitro*. *Lab. Invest.* **74**, 374–383
26. LeVine, H, III.. (1997) Stopped-flow kinetics reveal multiple phases of thioflavin T binding to Alzheimer β(1-40) amyloid fibrils. *Arch. Biochem. Biophys.* **342**, 306–316
27. Hamada, D. and Dobson, C.M. (2002) A kinetic study of β-lactoglobulin amyloid fibril formation promoted by urea. *Protein Sci.* **11**, 2417–2426
28. Ban, T., Hamada, D., Hasegawa, K., Naiki, H., and Goto, Y. (2003) Direct observation of amyloid fibril growth monitored by thioflavin T fluorescence. *J. Biol. Chem.* **278**, 16462–16465
29. Boshuizen, R.S., Langeveld, J.P.M., Salmona, M., Williams, A., Meloen, R.H., and Langedijk, J.P.M. (2004) An in vitro screening assay based on synthetic prion protein peptides for identification of fibril-interfering compounds. *Anal. Biochem.* **333**, 372–380
30. Beher, D., Hesse, L., Masters, C.L., and Multhaup, G. (1996) Regulation of amyloid protein precursor (APP) binding to collagen and mapping of the binding sites on APP and collagen type I. *J. Biol. Chem.* **271**, 1613–1620
31. Relini, A., Canale, C., De Stefano, S., Rolandi, R., Giorgetti, S., Stoppini, M., Rossi, A., Fogolari, F., Corazza, A., Esposito, G., Gliozzi, A., and Bellotti, V. (2006) Collagen plays an active role in the aggregation of β2-microglobulin under physio-pathological conditions of

dialysis-related amyloidosis. *J. Biol. Chem.* **281**, 16521–16529
32. Kalaria, R. and Pax, A.B. (1995) Increased collagen content of cerebral microvessels in Alzheimer's disease. *Brain. Res.* **705**, 349–352
33. Morimoto, K., Furuta, E., Hashimoto, H., and Inouye, K. (2006) Effects of high concentration of salts on the esterase activity and structure of a kiwifruit peptidase, actinidain. *J. Biochem.* **139**, 1065–1071
34. Morimoto, K., Kunii, S., Hamano, K., and Tonomura, B. (2004) Preparation and structural analysis of actinidain-processed atelocollagen of yellowfin tuna (*Thunnus albacares*). *Biosci. Biotechnol. Biochem.* **68**, 861–867
35. Laemmli, U.K. (1970) Cleavage of structural proteins during the assembly of the head of bacteriophage T4. *Nature* **227**, 680–685
36. Brown, F.R. III, Corato, A., Lorenzi, G.P., and Blout, E.R. (1972) Synthesis and structural studies of two collagen analogues: poly(L-prolyl-L-seryl-glycyl) and poly(L-prolyl-L-alanyl- glycyl). *J. Mol. Biol.* **63**, 85–99
37. Kuznetsova, N.V., McBride, D.J. Jr, and Leikin, S. (2003) Change in thermal stability and microunfolding pattern of collagen helix resulting from the loss of α2(I) chain in osteogenesis imperfecta murine. *J. Mol. Biol.* **331**, 191–200
38. Wisniewski, T., Castaño, E.M., Golabek, A., Vogel, T., and Frangione, B. (1994) Acceleration of Alzheimer's fibril formation by apolipoprotein E *in vitro*. *Am. J. Pathol.* **145**, 1030–1035
39. Sweeney, S.M., Orgel, J.P., Fertala, A., McAuliffe, J.D., Turner, K.R., Di Lullo, G.A., Chen, S., Antipova, O., Perumal, S., Ala-Kokko, L., Forlino, A., Cabral, W.A., Barnes, A.M., Marini, J.C., and San Antonio, J.D. (2008) Candidate cell and matrix interaction domains on the collagen fibril, the predominant protein of vertebrates. *J. Biol. Chem.* **283**, 21187–21197